STM JOURNALS

Research & Reviews: Journal of
Computational Biology

https://journals.stmjournals.com/rrjocb

ISSN: 2319-3433 (Online)
ISSN: 2349-3720 (Print)
Volume 13, Issue 2, 2024
May–August
DOI (Journal): 10.37591/RRJoCB

Research RRJoCB

In Silico Molecular Docking Studies of Phytocompounds from *Melissa officinalis* Against MPXV Poxin Target

Charith R.[1,*]

Abstract

Objectives: *This study aimed to evaluate the inhibitory potential of phytocompounds of Melissa officinalis against the MPXV poxin protein target, a key virulence factor in monkeypox infection.* ***Methods:*** *Molecular docking performed using PyRx, a virtual screening software, was conducted to predict the binding affinities of the compounds to MPXV poxin. Prior to docking, the compounds were subjected to comprehensive analysis, including Lipinski's rule of five, evaluation of physicochemical properties, pharmacological analysis using SwissADME, and toxicity analysis using pkCSM.* ***Results:*** *The results highlighted caryophyllenol II as the most promising inhibitor, with a binding affinity of -6.7 kcal/mol, suggesting a strong interaction with the target protein. Geranic acid also exhibited notable binding affinity, but to a lesser extent.* ***Conclusion:*** *Caryophyllenol II emerged as a lead compound for further development as an antiviral agent against monkeypox due to its better binding affinity to MPXV poxin. These findings show the potential of natural phytocompounds as therapeutic agents against viral infections and contribute to the ongoing efforts in antiviral drug discovery.*

Keywords: MPXV poxin, Ramachandran plot, molecular docking, phytocompound, ADMET analysis, ligand interaction

INTRODUCTION

Many outbreaks of diseases can spread between animals and humans in the 21st century. These outbreaks happened because of recent developments like changes in the climate, how animals are taken care of, and contact between wild animals and humans. These infections from animals caused different illnesses, and some of them, like Marburg virus disease, Ebola, and SARS-CoV-2, led to more people dying than usual [1]. Monkeypox is a zoonotic viral infection caused by a double-stranded DNA virus, which is a member of the orthopoxvirus genus, which includes other viruses like smallpox and vaccinia. The disease was first found in 1958 among monkeys when shipped from Singapore to Denmark [2]. The first time humans got sick with monkeypox was in 1970 in the Democratic Republic of the Congo. After the first incidence, there were sometimes outbreaks in a few countries in West and Central Africa [3]. From May 13, 2022, the virus started spreading at the community level, and by the month of November 2022, more than 7,8000 cases appeared in over 100 countries, and thus the WHO made the disease a global health emergency [4]. WHO gave the new name as MPox for monkeypox disease in 2022 [5]. As of 4 February 2024, there have been a total of 93,937 confirmed cases and 179 deaths in over 113 countries.

DNA viruses usually copy and use their genetic material inside the cell nucleus, relying a lot on cell proteins. But poxviruses are different; they do not follow this pattern [6]. Poxviruses are unique because they depend a lot on proteins made by the virus itself to copy themselves inside the cell's cytoplasm [7]. Due to the large genome size of the MPox virus, it becomes challenging for the virus to

***Author for Correspondence**
Charith R.
E-mail: charithchari50@gmail.com

[1]Student, Department of Bioinformatics, University of Agricultural Sciences, Gandhi Krishi Vignana Kendra, Bengaluru, Karnataka, India

Received Date: May 20, 2024
Accepted Date: October 01, 2024
Published Date: November 04, 2024

Citation: Charith R. In Silico Molecular Docking Studies of Phytocompounds from *Melissa officinalis* Against MPXV Poxin Target. Research & Reviews: Journal of Computational Biology. 2024; 13(2): 25–38p.

penetrate host defenses, and achieving rapid replication becomes a significant challenge. Consequently, the virus must devise alternative strategies to ensure its survival within the host. The individual's immune system is triggered early by the virus's large genome size, prompting immediate immune reactions [8, 9]. The proteins virotransducer and virostealth possess the capability to exert modulatory functions against the host immune system. Virotransducers are proteins that disrupt the host cell's response to infection, while virostealth proteins diminish the virus's detectability by the host immune system. These proteins achieve this by suppressing immune recognition molecules like MHC class I and CD4+, thereby reducing the likelihood of an immune response against the virus [7–9]. These modulatory proteins work together to avoid detection and attack by the host's immune system and play a crucial role in allowing the virus to replicate within the host's cytoplasm. Without these proteins, the virus would be vulnerable to the immune response and would not be able to survive and replicate effectively [10].

Most people who get monkeypox get better without needing medicine. Some might need help with their symptoms, like drinking fluids by mouth or through a tube, taking medicine for pain, or getting antibiotics for other infections [11]. However, treatment is recommended for patients with severe illness; those at high risk of getting worse, or those with skin or eye infections [12]. As both smallpox and monkeypox are from the same group of viruses called orthopoxviruses, medicines used to treat smallpox like brindidofovir, tecovirimat, and cidofovir are also considered for treating monkeypox [13]. Tecovirimat is the top treatment for smallpox and has proven to work against similar viruses like monkeypox [12]. Although there is not a vaccine specifically made to stop monkeypox right now, the information shows that vaccines like ACAM2000 and JYNNEOS, which are used for smallpox, might help protect against monkeypox. They could also make a monkeypox infection less severe [14]. Scientists are looking into different treatments because antiviral drugs can have side effects and viruses are getting better at resisting them. They are checking out herbal medicines as an option because they can fight viruses too. These herbal treatments are safer, cheaper, and easier to find [15, 16].

Melissa officinalis, also known as lemon balm, as shown in Figure 1, is a type of plant found in the Plantae kingdom. It belongs to the *Leguminosae* family and is classified as an angiosperm. Lemon balm is a popular herbal medicine used to treat various disorders, including gastrointestinal issues. Additionally, it is valued for its ability to relieve gas, muscle spasms, and pain, as well as promote relaxation and boost energy levels. Many people also believe that lemon balm has antioxidant [17] and antiviral effects [18]. Furthermore, numerous studies have highlighted the ability of *Melissa officinalis* to combat various viruses, including HSV-1 [18], CPV [19], HBV [20], and HCV [21]. These findings confirm its effectiveness as an alternative treatment for several viral infections.

Melissa officinalis contains a diverse array of chemical compounds, including terpenes, aldehydes, ketones, alcohols, oxides, esters, acids, and other miscellaneous compounds. These compounds are associated with various biological activities [22]. Many of these compounds have been found to exhibit antiviral effects. Due to their antiviral properties, these compounds are often considered as potential ligands in drug discovery. In today's world, creating new medicines often involves using computers. Scientists use special computer programs to find the best versions of potential drugs and to search for promising candidates. This method, called virtual screening, is more efficient and cost-effective compared to traditional methods, helping scientists to find potential drugs faster and cheaper [23].

MATERIALS AND METHODS

Retrieval and Preparation of Protein Target

The 3D crystal structure of the MPXV poxin classified as a viral protein, with Protein Data Bank (PDB) ID:8C9K, was retrieved from a protein structural database called RCSB Protein Data Bank (https://www.rcsb.org/) [24]. The crystal structure, determined using X-ray diffraction, has a resolution of 1.72 Å and does not contain any mutations. The crystal structure was then visualized using Discovery Studio Visualizer (https://discover.3ds.com/discovery-studio-visualizer-download) and the water molecules and heteroatoms were removed to make sure to obtain the purified protein [25]. The processed 3D protein was saved in PDB format for molecular docking studies.

Figure 1. *Melissa officinalis.*

Protein Structure Analysis

With the help of the PDBsum (*https://www.ebi.ac.uk/thornton-srv/databases/pdbsum/*) database that provides detailed structural and functional information on macromolecules in the PDB. The protein structure analysis encompassed multiple aspects to elucidate the structural characteristics and functional insights of MPXV poxin. Firstly, secondary structure analysis was conducted to delineate the architectural features of the protein. This analysis provided a comprehensive overview of the protein's structural elements [26]. Subsequently, interfacial analysis was performed to investigate the interactions between the protein chains. Interface analysis revealed the number of interface residues, interface area, presence of salt bridges, disulphide bonds, hydrogen bonds, and non-bonded contacts, shedding light on the inter-chain interactions within the protein assembly. Finally, structural validation was carried out using Ramachandran plot analysis obtained from PROCHECK. The Ramachandran plot statistics provided insights into the conformational quality and stereochemical integrity of the protein structure [27].

Ligand Selection and Preparation

The phytocompounds of *Melissa officinalis* chosen from the Indian medicinal plants, phytochemistry and therapeutics 2.0 (IMPPAT 2.0) webserver (*https://cb.imsc.res.in/imppat/*), were identified within medicinal plants, and their 3D structures were retrieved in structure-data file (SDF) format from PubChem (*http://pubchem.ncbi.nlm.nih.gov/*).

ADME Analysis

In our study, we utilized SwissADME (*http://www.swissadme.ch/*), an online tool, to evaluate the physicochemical properties, pharmacokinetics, and drug-likeness of the compounds under investigation. The chemical structures of the ligands, obtained from PubChem, were inputted into SwissADME in the form of Canonical SMILES. We applied Lipinski's rule of five to determine the drug-likeness of the compounds, ensuring they adhere to established criteria for oral bioavailability and permeation [28], as shown in Table 1. Additionally, we assessed the parameters of physicochemical characteristics, as depicted in Table 2. Furthermore, we analyzed pharmacokinetic properties such as gastrointestinal absorption, blood-brain barrier (BBB) permeability, and the potential interactions of molecules with cytochrome P450 (CYP) enzyme parameters as shown in Table 3. This superfamily of isoenzymes plays a crucial role in drug elimination through metabolic biotransformation. It has been suggested that CYP and P-glycoprotein (P-gp) can process small molecules synergistically to improve the protection of tissues and organisms. It helped to assess the potential effectiveness and distribution of the compounds within the body. The insights obtained from SwissADME informed our decision-making process regarding compound selection and optimization strategies in our study, enriching our understanding of their pharmacological potential.

Table 1. Lipinski's rule of five parameters.

Parameters	Optimal range
Molecular weight	<500 Daltons
MlogP	<4.15
H Donors	<10
H acceptors	<5
Molecular refractivity	40–130

MlogP: Molecular Logarithm of the Partition Coefficient

Table 2. Parameters for physiochemical properties.

Parameters		Optimal range
Lipophilicity	xLogP	-0.7–+5.0
Size	Molecular weight	150–500 g/mol
Polarity	TPSA	20–130
Saturation	Sp3 hybridization	>0.25
Flexibility	Rotatable bonds (RB)	<10

Toxicity

In our study, we employed the pkCSM tool (*https://biosig.lab.uq.edu.au/pkcsm/prediction*) to evaluate the maximum recommended tolerated dose (MRTD) that serves as an estimate of the toxic dose threshold of chemicals in human. The MRTD is a crucial parameter that helps us understand the potential toxicity of the compounds under investigation. An MRTD value of <=0.477 (log mg/kg/day) is indicative of low toxicity, suggesting that the compound may have minimal adverse effects at typical exposure levels. By considering the MRTD in our analysis, we aim to prioritize compounds with favorable safety profiles for further investigation. This approach allows us to identify and focus on compounds that hold promise for therapeutic development while minimizing the risk of harmful effects on human health.

Molecular Docking

Molecular docking was performed to explore how phytochemical compounds interact with the MPXV poxin protein target, using a tool called PyRx 0.8 (*https://sourceforge.net/projects/pyrx/*) [29]. PyRx is an open-access and user-friendly software that combines several open-source programs, including AutoDock, AutoDock Vina, and Open Babel, to conduct docking studies [29].

Before starting the docking process, we first prepared the protein structure by considering all its chains (A, B, C, and D) to capture its complete structure. Then, we converted this protein structure from pdb to pdbqt format suitable for docking using the Auto Dock Tools utility.

Similarly, we obtained the phytochemical compounds of *Melissa officinalis* and made sure their 3D structures were optimized by minimizing their energy. This step was important to ensure that the compounds were in their best shape for docking. Then, we converted these compound structures from SDF to pdbqt format suitable for docking using a tool called Open Babel.

The active site of the protein is unknown, and we covered the entire protein with a grid to maximize the search space. The grid encompasses the entire protein structure, allowing the ligand to explore potential binding sites across the entire protein surface [30]. The docking parameters were set with an exhaustive value of 8 to ensure a thorough exploration of binding poses. The grid center coordinates were specified as center_x = 1.0234, center_y = 1.9524, and center_z = -67.7596, with dimensions of size_x = 87.4437791061, size_y = 56.3557398987, and size_z = 100.707220688 in the X, Y, and Z directions, respectively. This comprehensive grid setup facilitated an extensive search for potential binding interactions between the ligands and the MPXV poxin target, aiding in the identification of promising binding sites for further analysis.

Finally, we ran the docking using PyRx with the AutoDock Vina docking engine. This software calculates how well the compounds fit into the defined search area and predicts how strongly they might bind to the protein. The graphical visualization of docking results was done by using BIOVIA Discovery software to understand how the compounds interacted with the protein and where they might attach [31].

RESULTS

Protein Preprocessing

The crystal structure of the protein MPXV poxin target with PBD_ID: 8C9K protein model was selected and downloaded in the PDB file format as shown in Figure 2(a). The three-dimensional structure of the protein was prepared for molecular docking by following a protein purification using the BIOVIA Discovery Studio tool. By purifying the protein, its integrity, and suitability for docking studies are ensured, thus enhancing the reliability and interpretability of the docking results for docking studies, which is shown in Figure 2(b).

Protein Structure Analysis

The crystal structure of MPXV poxin reveals a tetrameric assembly with four chains labeled A, B, C, and D, each consisting of 194 residues. Analysis of the secondary structure reveals a complex architecture, characterized by a total of 7 sheets, 8 beta hairpins, 7 beta bulges, and 20 strands, indicative of extensive beta-sheet formation. Additionally, the structure exhibits 3 helices, contributing to its overall tertiary fold. Notably, the presence of 16 beta turns and 1 gamma turn further highlights the structural diversity within the protein. These secondary structure elements collectively contribute to the stabilization and functional organization of MPXV poxin, as depicted in Figure 3.

Interfacial Analysis

The interface analysis of MPXV poxin reveals diverse interaction patterns between its chains. Notably, Interface A-chain and B-chain exhibit 22 interface residues with an interface area of 1069 Å², featuring 2 salt bridges while lacking disulphide bonds. Additionally, it comprises 18 hydrogen bonds and 137 non-bonded contacts. In contrast, Interface A-chain and C-chain comprise 3 interface residues, with a smaller interface area of 326 Å², and are devoid of disulphide bonds. This interface showcases 3 hydrogen bonds. Finally, Interface C-chain and D-chain involve 4 interface residues, spanning an interface area of 279 Å², with 1 salt bridge. Although this interface lacks disulphide bonds, it presents 3 hydrogen bonds. These findings elucidate the diverse interaction profiles between MPXV poxin chains, shedding light on their structural integrity and functional implications (Figure 4).

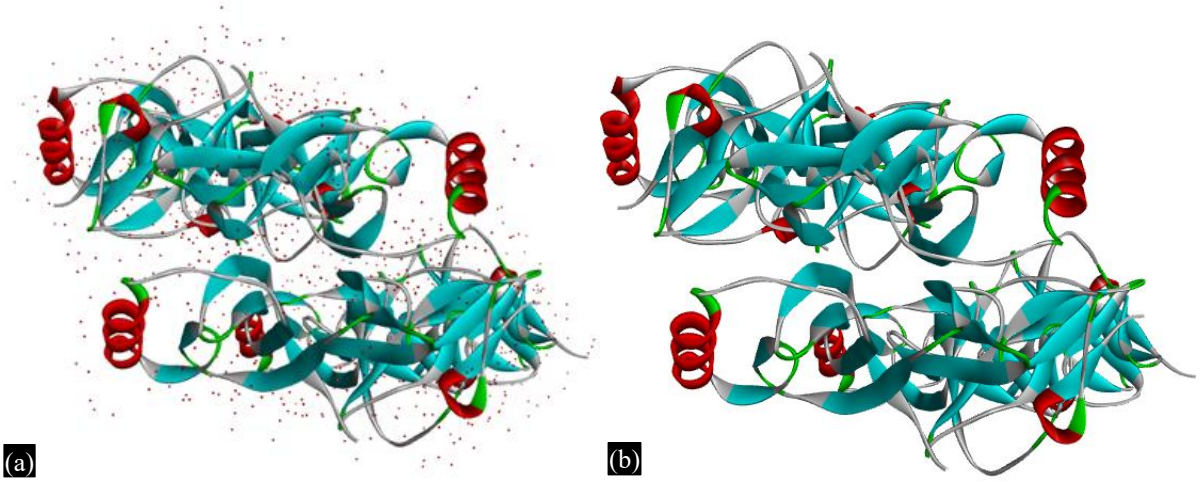

Figure 2. (a) 3D structure of MPXV poxin protein. (b) 3D structure of purified MPXV poxin protein.

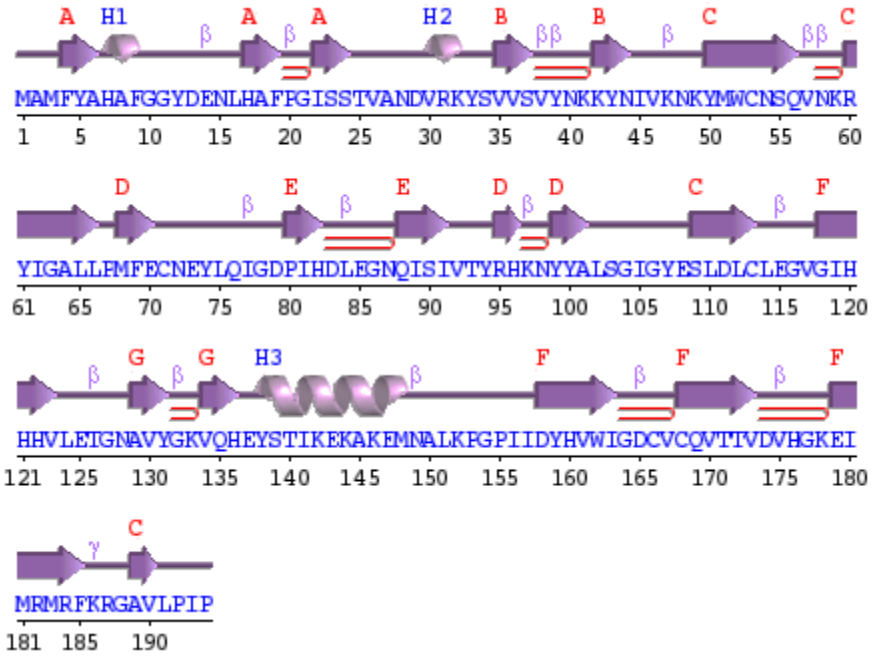

Figure 3. Secondary structure of MPXV poxin.

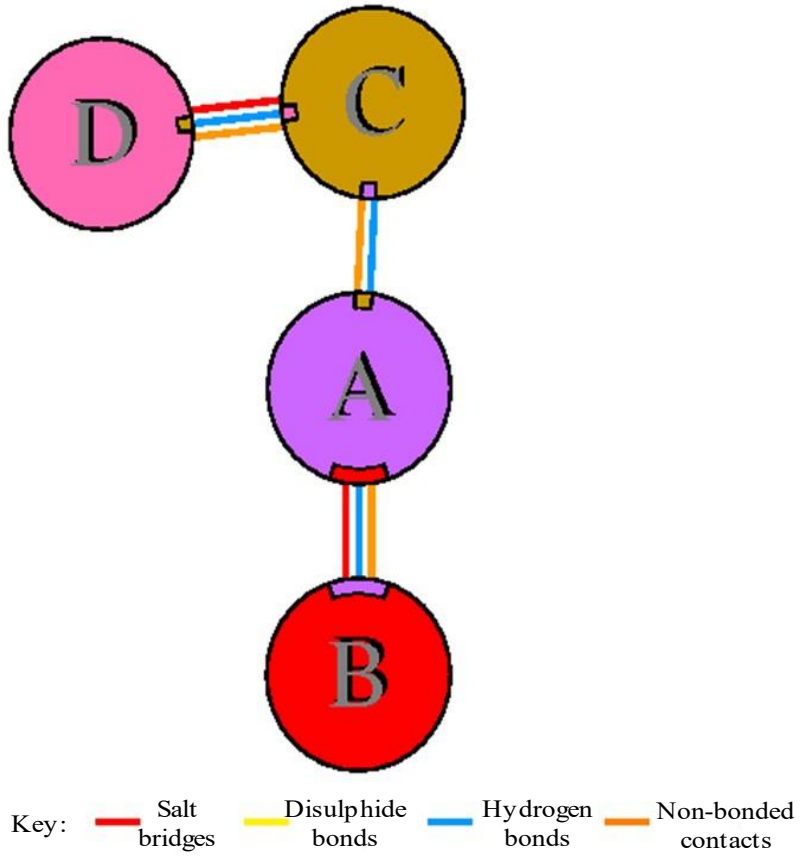

Figure 4. Schematic diagram of interactions between protein chains.

Structural Validation

The structural validation of the MPXV poxin protein structure using Ramachandran plot analysis reveals favorable statistics indicative of its high quality. The plot illustrates the distribution of residues

within different regions of the plot, with a significant portion (90.0%) falling within the most favored regions. Additionally, a small percentage (9.1%) of residues are found within the additional allowed regions. Only a negligible fraction of residues (0.3%) occupies the generously allowed regions, demonstrating minimal deviation from ideal structural conformations. Notably, a small percentage (0.6%) of residues are located in disallowed regions, suggesting limited structural irregularities. Overall, the structural integrity of MPXV poxin is upheld, with all non-glycine and non-proline residues (100.0%) meeting validation criteria. The analysis includes end-residues (excluding Gly and Pro) totaling 4, along with 64 glycine residues and 28 proline residues, contributing to a total of 776 residues in the protein structure. These findings underscore the robustness of the MPXV poxin structure, validating its suitability for further functional and computational studies (Figure 5).

Collection of Phytochemical Compounds

30 phytochemical compounds of *Melissa officinalis* such as beta-bisabolene; octanal; 6,10,14-trimethylpentadecan-2-one; carvacrol; decane; 3-octanol; pinocarvone; 2-(4-methylphenyl) propan-2-ol; myrcene; diacetone alcohol; coumarin; eugenol; bicyclogermacrene; trans-1(7),8-p-menthadien-2-ol; caryophyllenol II; labd-14-ene, 8,13-epoxy-, (13S)-; beta-guaiene; (-)-beta-bourbonene; gamma-terpinene; geranyl formate; geranic acid; 1,3,3-trimethyl-2-oxabicyclo[2.2.2] oct-5-ene; stearic acid; 3-(methylthio)propionaldehyde; 1-octen-3-OL; p-cymene; methyl geranate; myrtenal; nerol oxide; 6-methyl-3,5-heptadien-2-one sourced from the IMPPAT database were selected for analysis in this study.

Lipinski's Rule of Five Analysis

The selected 30 compounds were subjected to evaluation against Lipinski's rule of five using the SwissADME webserver. Following rigorous analysis, it was found that only 21 compounds successfully met the criteria of zero violation of Lipinski's rule, demonstrating favorable drug-like properties, and the remaining 9 compounds, such as beta-bisabolene, 6,10,14-trimethylpentadecan-2-one, decane, bicyclogermacrene, labd-14-ene 813-epoxy- (13S)-, beta-guaiene, (-)-beta-bourbonene, stearic acid, p-cymene exhibit violation of Lipinski's rule. The results of this assessment are presented in (Table 3).

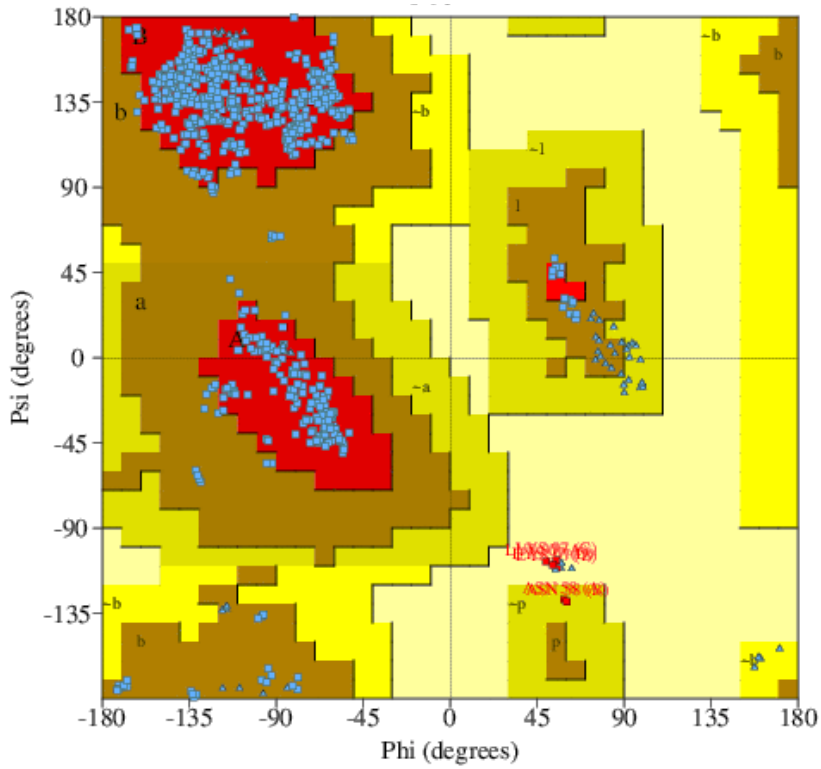

Figure 5. Ramachandran plot of MPXV poxin protein.

Table 3. Data for the properties of the Lipinski was obtained using SwissADME.

Ligand	Formula	MW	MLOGP	H acceptors	H donors	MR	Violation (0/1)
Beta-bisabolene	$C_{15}H_{24}$	204.35	4.53	0	0	70.68	1
Octanal	$C_8H_{16}O$	128.21	2.07	1	0	40.77	0
6,10,14-trimethylpentadecan-2-one	$C_{18}H_{36}O$	268.48	4.79	1	0	88.84	1
Carvacrol	$C_{10}H_{14}O$	150.22	2.76	1	1	48.01	0
Decane	$C_{10}H_{22}$	142.28	4.82	0	0	50.18	1
3-octanol	$C_8H_{18}O$	130.23	2.22	1	1	41.73	0
Pinocarvone	$C_{10}H_{14}O$	150.22	2.2	1	0	45.42	0
2-(4-methylphenyl) propan-2-ol	$C_{10}H_{14}O$	150.22	2.49	1	1	47.03	0
Myrcene	$C_{10}H_{16}$	136.23	3.56	0	0	48.76	0
Diacetone alcohol	$C_6H_{12}O_2$	116.16	0.46	2	1	32.36	0
Coumarin	$C_9H_6O_2$	146.14	1.65	2	0	42.48	0
Eugenol	$C_{10}H_{12}O_2$	164.2	2.01	2	1	49.06	0
Bicyclogermacrene	$C_{15}H_{24}$	204.35	4.63	0	0	68.78	1
trans-1(7),8-p-menthadien-2-ol	$C_{10}H_{16}O$	152.23	2.2	1	1	48.28	0
Caryophyllenol II	$C_{15}H_{24}O$	220.35	3.56	1	1	69.94	0
Labd-14-ene, 8,13-epoxy-, (13S)-	$C_{20}H_{34}O$	290.48	4.86	1	0	92.08	1
Beta-guaiene	$C_{15}H_{24}$	204.35	4.63	0	0	69.04	1
(-)-beta-bourbonene	$C_{15}H_24$	204.35	5.65	0	0	67.14	1
Gamma-Terpinene	$C_{10}H_{16}$	136.23	3.27	0	0	47.12	0
Geranyl formate	$C_{11}H_{18}O_2$	182.26	2.67	2	0	55.72	0
Geranic acid	$C_{10}H_{16}O_2$	168.23	2.38	2	1	51.01	0
1,3,3-trimethyl-2-oxabicyclo [2.2.2] oct-5-ene	$C_{10}H_{16}O$	152.23	2.3	1	0	46.64	0
Stearic acid	$C_{18}H_{36}O_2$	284.48	4.67	2	1	90.41	1
3-(methylthio) propionaldehyde	C_4H_8OS	104.17	0.6	1	0	29.13	0
1-Octen-3-OL	$C_8H_{16}O$	128.21	2.07	1	1	41.26	0
p-Cymene	$C_{10}H_{14}$	134.22	4.47	0	0	45.99	1
Methyl geranate	$C_{11}H_{18}O_2$	182.26	2.67	2	0	55.33	0
Myrtenal	$C_{10}H_{14}O$	150.22	2.2	1	0	45.42	0
Nerol oxide	$C_{10}H_{16}O$	152.23	2.2	1	0	48.21	0
6-Methyl-3,5-heptadien-2-one	$C_8H_{12}O$	124.18	1.87	1	0	39.82	0

MW: Molecular weight, MR: Molecular refractivity

Physicochemical Analysis

Physicochemical analysis was conducted on the 21 phytochemical compounds from *Melissa officinalis* that successfully passed Lipinski's rule of five, as depicted in (Table 3). Parameters such as molecular weight, hydrogen bond donors, hydrogen bond acceptors, logP (lipophilicity), polar surface area, Csp3 hybridization, and the number of rotatable bonds were evaluated using SwissADME. Among the 21 compounds, 3-(methylthio) propionaldehyde, diacetone alcohol, 6-methyl-3,5-heptadien-2-one, octanal, 1-octen-3-OL, 3-octanol, myrcene, gamma-terpinene, and coumarin, with molecular weights of 104.17, 116.16, 124.18, 128.21, 128.21, 130.23, 136.23, 136.23, and 146.14, respectively, did not meet the parameters outlined in (Table 2). Additionally, the compound eugenol exhibited a fraction Csp3 of 0.2, which did not meet the parameters specified in (Table 2). Similarly, pinocarvone, myrtenal, 1,3,3-trimethyl-2-oxabicyclo [2.2.2] oct-5-ene, and nerol oxide displayed total polar surface area (TPSA) values of 17.07, 17.07, 9.23, and 9.23, respectively, which also did not meet the criteria set forth in (Table 2). Only 7 met the physicochemical parameters crucial for pharmacokinetic behavior and potential drug-likeness. The results of this analysis are presented in (Table 4).

Table 4. Physiochemical properties obtained using SwissADME.

Ligand	MW	Fraction Csp3	RB	TPSA	Lipophilicity
Octanal	128.21	0.88	6	17.07	2.72
Carvacrol	150.22	0.4	1	20.23	3.49
3-octanol	130.23	1	5	20.23	2.78
Pinocarvone	150.22	0.7	0	17.07	2.16
2-(4-methylphenyl) propan-2-ol	150.22	0.4	1	20.23	1.99
Myrcene	136.23	0.4	4	0	4.17
Diacetone alcohol	116.16	0.83	2	37.3	-0.19
Coumarin	146.14	0	0	30.21	1.39
Eugenol	164.2	0.2	3	29.46	2.27
trans-1(7), 8-p-menthadien-2-ol	152.23	0.6	1	20.23	2.3
Caryophyllenol II	220.35	0.73	0	20.23	3.08
Gamma-terpinene	136.23	0.6	1	0	4.5
Geranyl formate	182.26	0.55	6	26.3	4.15
Geranic acid	168.23	0.5	4	37.3	3.09
1,3,3-trimethyl-2-oxabicyclo [2.2.2] oct-5-ene	152.23	0.8	0	9.23	1.89
3-(methylthio) propionaldehyde	104.17	0.75	3	42.37	0.31
1-octen-3-OL	128.21	0.75	5	20.23	2.55
Methyl geranate	182.26	0.55	5	26.3	3.42
Myrtenal	150.22	0.7	1	17.07	2.98
Nerol oxide	152.23	0.6	1	9.23	2.22
6-methyl-3,5-heptadien-2-one	124.18	0.38	2	17.07	2.04

TPSA: Total Polar Surface Area

Pharmacokinetic Analysis

The 7 phytochemical compounds from Melissa officinalis that passed Lipinski's rule of five and physicochemical parameters were further subjected to pharmacokinetic analysis using SwissADME.

Parameters such as gastrointestinal absorption, BBB permeability, and interactions with cytochrome P450 (CYP) enzymes were assessed to evaluate the compounds' pharmacokinetic properties. Carvacrol and 2-(4-methylphenyl) propan-2-ol exhibit CYP1A2 inhibitor, which is a key enzyme involved in the metabolism of various endogenous compounds and xenobiotics, including drugs, toxins, and carcinogens. Inhibition of CYP1A2 activity can lead to alterations in the metabolism of co-administered drugs, potentially resulting in drug-drug interactions and adverse effects [32]. Additionally, CYP1A2 inhibition has been implicated in modulating the bioavailability and pharmacokinetics of drugs, affecting their therapeutic efficacy and safety profiles and the results depicted in Table 5. Only 5 compounds were subjected to toxicity prediction.

Table 5. Pharmacokinetic analysis.

Ligand	GI absorption	BBB permeant	P-gp substrate	CYP1A2 inhibitor	CYP2C19 inhibitor	CYP2C9 inhibitor	CYP2D6 inhibitor	CYP3A4 inhibitor
Carvacrol	High	Yes	No	Yes	No	No	No	No
2-methylphenyl) propan-2-ol	High	Yes	No	Yes	No	No	No	No
trans-1(7),8-p-menthadien-2-ol	High	Yes	No	No	No	No	No	No
Caryophyllenol II	High	Yes	No	No	No	No	No	No
Geranyl formate	High	Yes	No	No	No	No	No	No
Geranic acid	High	Yes	No	No	No	No	No	No
Methyl geranate	High	Yes	No	No	No	No	No	No

Toxicity Analysis

Toxicity analysis was conducted using the pkCSM tool to assess the potential adverse effects of the phytochemical compounds from *Melissa officinalis*. Ligands such as trans-1(7), 8-p-menthadien-2-ol; geranyl formate; and methyl geranate exhibited MRTD values of 0.901, 0.52, and 0.798, respectively, suggesting potential toxicity according to the toxicity assessment. Consequently, the remaining two phytochemical compounds were considered suitable for the molecular docking process, as detailed in Table 6.

Molecular Docking

Studies were conducted to assess the inhibitory potential of selected phytocompounds, namely caryophyllenol II and geranic acid, against the MPXV poxin protein. The results, including ligand interaction details, are presented in Table 7, which highlights the binding affinities of the compounds to MPXV poxin. Among the investigated compounds, caryophyllenol II demonstrated the highest binding affinity of -6.7 kcal/mol (caryophyllenol II_uff_E = 741.89_uff_E = 741.89), indicating a strong and robust interaction with the target protein, and geranic acid has the binding affinity of -5.3 kcal/mol, which is shown in Figure 6(a and b).

Table 6. Toxicity analysis.

Ligand	MRTD (log mg/kg/day) > = 0.477
trans-1(7),8-p-menthadien-2-ol	0.901
Caryophyllenol II	0.216
Geranyl formate	0.52
Geranic acid	0.312
Methyl geranate	0.798

Table 7. Docking results.

Target	Ligands	Binding affinity (kcal/mol)	Ligand interactions
8C9K	Caryophyllenol II_uff_E=741.89	-6.7	LYS C:41= AlkylTHR C:39 = Pi- AlkylLEU C:75 = Alkyl
8C9K	Geranic acid_uff_E=118.05	-5.3	LYS A:186 = Hydrogen HIS B:17 = Pi-AlkylPHE B:19 = Pi- AlkylALA B:27 = AlkylILE B:105 = Alkyl

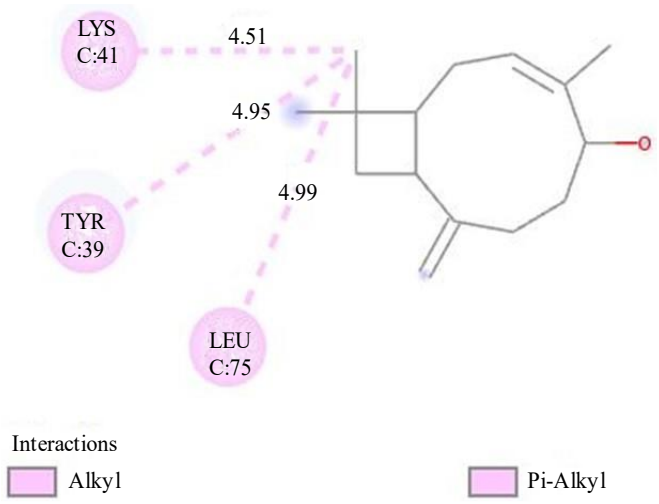

Figure 6. (a) 2D plot of complex caryophyllene II with 8C9K target

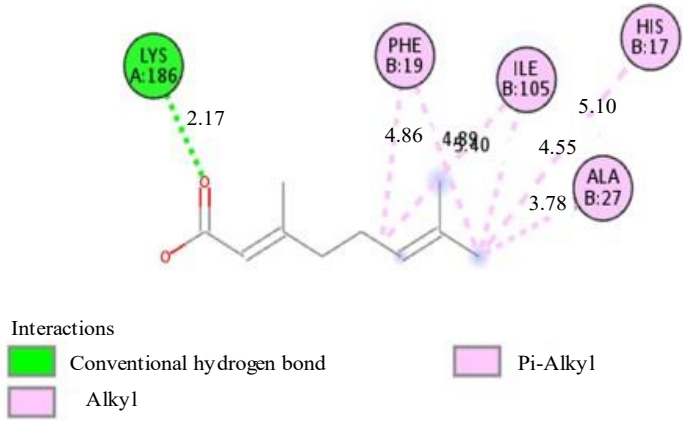

Figure 6. (b) 2D plot of complex geranic acid with 8C9K target.

DISCUSSION

The study aims to investigate the inhibitory potential of selected phytoconstituents against the MPXV poxin protein target. Prior to molecular docking, the protein structure underwent rigorous purification to ensure its integrity and suitability for docking studies. This purification process was conducted using the BIOVIA Discovery Studio tool. The high-quality structural validation of the MPXV poxin protein further supports the reliability of our findings. Analysis of the Ramachandran plot revealed a significant portion of residues of about 90 percent present within the most favored regions, indicating the protein's favorable conformational quality.

In this study, 30 phytochemical compounds sourced from *Melissa officinalis* were selected from the IMPPAT database. Lipinski's rule of five criteria was applied to assess the drug-likeness of these compounds, resulting in the identification of 21 compounds meeting the criteria and exhibiting favorable drug-like properties. Subsequent physicochemical analysis further narrowed down the selection to seven compounds demonstrating suitable pharmacokinetic behavior.

Pharmacokinetic analysis provided insights into the compounds' absorption, blood-brain barrier permeability, and interactions with cytochrome P450 enzymes. The compounds like carvacrol and 2-(4-methylphenyl) propan-2-ol exhibited CYP1A2 inhibition, which plays a significant role in drug metabolism and pharmacokinetics. CYP1A2 is involved in the metabolism of numerous drugs and xenobiotics, including caffeine, theophylline, and certain antidepressants [33]. Understanding the importance of CYP1A2 inhibition is crucial for predicting drug-drug interactions, optimizing dosing regimens, and ensuring safe and effective pharmacotherapy [34]. Only 5 compounds were subjected to toxicity prediction.

Toxicity assessment using the pkCSM tool identified potential adverse effects associated with certain compounds, leading to the exclusion of three compounds from further analysis. The remaining two compounds, like caryophyllenol II and geranic acid, were subjected to molecular docking studies to evaluate their inhibitory potential against the MPXV poxin protein.

Among the investigated compounds, caryophyllenol II demonstrated the highest binding affinity of -6.7 kcal/mol, indicating a strong interaction with the MPXV poxin protein. The ligand caryophyllenol II forms the interaction, with lysine (LYS) at position 41 in chain C through an alkyl interaction, and threonine (THR) at position 39 in chain C interacts through a pi-alkyl interaction. Pi-alkyl interactions involve the interaction between an aromatic system in the ligand and a hydrophobic group in the amino acid side chain and also leucine (LEU) at position 75 in chain C interacts through an alkyl interaction. Leucine residues are commonly involved in hydrophobic interactions due to their non-polar side chains.

Geranic acid also exhibited a notable binding affinity of -5.3 kcal/mol, which showed its potential as an inhibitor of MPXV poxin. The ligand geranic acid engages in specific interactions with amino acid residues within the protein structure, elucidating key molecular interactions essential for binding. At position 186 in chain A, geranic acid forms a hydrogen bond with lysine (LYS), highlighting the potential for hydrogen bonding interactions facilitated by the positively charged side chains of lysine residues. In chain B, histidine (HIS) at position 17 and phenylalanine (PHE) at position 19 participate in pi-alkyl interactions with geranic acid, indicating the involvement of aromatic systems in hydrophobic interactions with the ligand. Additionally, alanine (ALA) at position 27 and isoleucine (ILE) at position 105 form alkyl interactions with geranic acid, underscoring the contribution of non-polar side chains to hydrophobic interactions. These specific interactions between caryophyllenol II and amino acid residues and geranic acid and amino acid residues of protein targets provide valuable insights into the molecular basis of ligand-protein binding, which can inform drug design strategies aimed at optimizing binding affinity and specificity.

CONCLUSION

In summary, our research has showcased the significant promise of caryophyllenol II_uff_E = 741.89 as a potential inhibitor for MPXV poxin, a crucial therapeutic target associated with the MPox virus. From molecular docking studies, caryophyllenol II demonstrated the highest binding affinity of -6.7 kcal/mol among all the investigated phytocompounds of *Melissa officinalis*. The next phase of our research involves extending the docking studies to explore the interactions of these phytocompounds with other targets associated with the MPox virus. Additionally, we plan to conduct molecular simulation studies to explain the dynamic behavior and stability of the ligand-protein complexes. This integrated approach will provide valuable insights into the potential therapeutic applications of these compounds against various targets implicated in MPox virus infection, paving the way for the development of novel antiviral agents.

Acknowledgment

I express my gratitude to the Department of Bioinformatics, BioNome, located in Bengaluru, India, for granting access to their computational facilities and offering support during this scientific research. I extend my appreciation to Ms. Samiksha Bhor for her invaluable assistance throughout the project.

Abbreviation

ADME: Adsorption Distribution Metabolism Excretion
CD4+: Cluster of Differentiation 4 positive
MHC class I: Major Histocompatibility Complex class I
MPXV: Monkeypox Virus
P-gp: Permeability Glycoprotein
RCSB: Research Collaboratory for Structural Bioinformatics
SMILES: Simplified Molecular Input Line Entry System

REFERENCES

1. Sallam M, Eid H, Awamleh N, Al-Tammemi AA, Barakat M, Athamneh RY, et al. Conspiratorial attitude of the general public in Jordan towards emerging virus infections: a cross-sectional study amid the 2022 Monkeypox outbreak. Trop Med Infect Dis. 2022;7(12):411. doi:10.3390/tropicalmed7120411.
2. Magnus PV, Andersen EK, Petersen KB, Birch-Andersen A. A pox-like disease in cynomolgus monkeys. Acta Pathol Microbiol Scand. 1959;46:156–176.
3. Nguyen PY, Ajisegiri WS, Costantino Vs, Chughtai AA, MacIntyre CR. Reemergence of human monkeypox and declining population immunity in the context of urbanization, Nigeria, 2017–2020. Emerg Infect Dis. 2021;27(4):1007–1014. doi:10.3201/eid2704.203569.
4. Karagoz A, Tombuloglu H, Alsaeed M, Tombuloglu G, AlRubaish AA, Mahmoud A, Smajlović S, Ćordić S, Rabaan AA, Alsuhaimi E. Monkeypox (mpox) virus: Classification, origin, transmission, genome organization, antiviral drugs, and molecular diagnosis. J Infect Public Health. 2023;16(4):531–541. doi:10.1016/j.jiph.2023.02.003.

5. Who.int. (2022). WHO recommends new name for monkeypox disease [Online]. World Health Organization. Available from: https://www.who.int/news/item/28-11-2022-who-recommends-new-name-for-monkeypox-disease.
6. Moss B. Poxvirus cell entry: how many proteins does it take?. Viruses. 2012;4(5):688–707. doi:10.3390/v4050688.
7. McInnes CJ, Damon IK, Smith GL, McFadden G, Isaacs SN, Roper RL, Evans DH, Damaso CR, Carulei O, Wise LM, Lefkowitz EJ. ICTV Virus taxonomy profile: poxviridae 2023. J Gen Virol. 2023;104(5):001849. doi:10.1099/jgv.0.001849.
8. Stanford MM, McFadden G, Karupiah G, Chaudhri G: Immunopathogenesis of poxvirus infections: forecasting the impending storm. Immunol Cell Biol. 2007;85(2):93–102. doi:10.1038/sj.icb.7100033.
9. Okyay RA, Bayrak E, Kaya E, Şahin AR, Koçyiğit BF, Taşdoğan AM, et al. Another epidemic in the shadow of Covid 19 pandemic: a review of monkeypox. EJMO. 2022;6(2):95–99. doi:10.14744/ejmo.2022.2022.
10. Petersen E, Kantele A, Koopmans M, Asogun D, Yinka-Ogunleye A, Ihekweazu C, Zumla A. Human monkeypox: epidemiologic and clinical characteristics, diagnosis, and prevention. Infect Dis Clin North Am. 2019;33(4):1027–1043. doi:10.1016/j.idc.2019.03.001.
11. Kang Y, Yu Y, Xu S. Human monkeypox infection threat: A comprehensive overview. PLOS Negl Trop Dis. 2023;17(4):E0011246. doi:10.1371/journal.pntd.0011246.
12. Huang Y, Mu L, Wang W. Monkeypox: epidemiology, pathogenesis, treatment and prevention. Signal Transduct Target Ther. 2022;7(1):373. doi:10.1038/s41392-022-01215-4.
13. Rizk JG, Lippi G, Henry BM, Forthal DN, Rizk Y. Prevention and treatment of monkeypox. Drugs. 2022 Jun;82(9):957-63.
14. Turner M, Mandia J, Keltner C, Haynes R, Faestel P, Mease L. Monkeypox in patient immunized with ACAM2000 smallpox vaccine during 2022 outbreak. Emerg Infect Dis. 2022;28(11):2336–2338. doi:10.3201/eid2811.221215.
15. Astani A, Heidary Navid M, Schnitzler P. Attachment and penetration of acyclovir-resistant herpes simplex virus are inhibited by Melissa officinalis extract. Phytother Res. 2014;28(10):1547–1552. doi:10.1002/ptr.5166.
16. Lee JY, Abundo ME, Lee CW. Herbal medicines with antiviral activity against the influenza virus, a systematic review. Am J Chin Med. 2018;46(08):1663–700. doi:10.1142/S0192415X18500854.
17. Miraj S, Rafieian-Kopaei, Kiani S. Melissa officinalis L: A Review study with an antioxidant prospective. J Evid Based Complement Altern Med. 2017;22(3):385–394. doi:10.1177/21565872166634.
18. Vanti G, Ntallis SG, Panagiotidis CA, Dourdouni V, Patsoura C, Bergonzi MC, Lazari D, Bilia AR. Glycerosome of Melissa officinalis L. essential oil for effective anti-HSV Type 1. Mol. 2020;25(14):3111. doi:10.3390/molecules25143111.
19. Williams A, Scally G, Langland J. A topical botanical therapy for the treatment of canine papilloma virus associated oral warts: a case series. Adv Integr Med. 2021;8(2):151–154. doi:10.1016/j.aimed.2020.12.003.
20. Astani A, Reichling J, Schnitzler P. Melissa officinalis extract inhibits attachment of herpes simplex virus in vitro. Chemotherapy. 2012;58(1):70–77. doi:10.1159/000335590.
21. Behzadi A, Imani S, Deravi N, Mohammad Taheri Z, Mohammadian F, Moraveji Z, Shavysi S, Mostafaloo M, Soleimani Hadidi F, Nanbakhsh S, Olangian-Tehrani S, Marabi MH, Behshood P, Poudineh M, Kheirandish A, Keylani K, Behfarnia P. Antiviral potential of Melissa officinalis L.: A literature review. Nutr Metab Insights. 2023;16:11786388221146683. doi:10.1177/11786388221146683.
22. Petrisor G, Motelica L, Craciun LN, Oprea OC, Ficai D, Ficai A. Melissa officinalis: Composition, pharmacological effects and derived release systems—A review. Int J Mol Sci. 2022;23(7):3591. doi.org/10.3390/ijms23073591.
23. Ahire SM, Jadhav SP, Shewale VV, Pawar PS, Kokande AM, Sonawane DP, Patil DM. A review on computer-aided drug design and discovery. J ReAttach Ther Dev Divers. 2023;6(10s(2)):1573–1582. doi:10.53555/jrtdd.v6i10s(2).2169.

24. Duchoslav V, Boura E. Structure of monkeypox virus poxin: implications for drug design. Arch Virol. 2023;168(7):192. doi:10.1007/s00705-023-05824-4.
25. Sastry GM, Adzhigirey M, Day T, Annabhimoju R, Sherman W. Protein and ligand preparation: parameters, protocols, and influence on virtual screening enrichments. J Comput Aided Mol Des. 2013;27(3):221–234. doi:10.1007/s10822-013-9644-8.
26. Fioramonte M, dos Santos AM, McIIwain S, Noble WS, Franchini KG, Gozzo FC. Analysis of secondary structure in proteins by chemical cross-linking coupled to MS. Prot. 2012;12(17):2746–2752. doi:10.1002/pmic.201200040.
27. Hollingsworth SA, Karplus PA. A fresh look at the Ramachandran plot and the occurrence of standard structures in proteins. Biomol Concepts. 2010;1(3-4):271–283. doi:10.1515/BMC.2010.022.
28. Chen X, Li H, Tian L, Li Q, Luo J, Zhang Y. Analysis of the physicochemical properties of acaricides based on Lipinski's rule of five. J Comput Biol. 2020;27(9):1397–1406. doi:10.1089/cmb.2019.03.
29. Kondapuram SK, Sarvagalla S, Coumar MS. Docking-Based Virtual Screening Using PyRx Tool: Autophagy Target Vps34 as a Case Study. In: Coumar MS, editor. Molecular Docking for Computer-Aided Drug Design. United States: Academic Press; 2021. 463–477. doi:10.1016/C2019-0-04960-6.
30. Sapjaroen P, Tangyuenyongwatana P. Study of steric factor on blind docking of phenylbutanoid dimers with PyRx 0.8 virtual screening tool. 35th International Annual Meeting in Pharmaceutical Sciences & CU-MPU International Collaborative Research Conference. Pathumthani, Thailand. 2019. 155–158. College of Oriental Medicine, Rangsit University.
31. Maurya VK, Kumar S, Singh M, Saxena V. Molecular docking and dynamic studies of novel phytoconstituents in an investigation of the potential inhibition of protein kinase C-beta II in diabetic neuropathy. J Mol Chem. 2023;3(2):589.
32. Lee J, Beers JL, Geffert RM, Jackson KD. A review of CYP-mediated drug interactions: mechanisms and In vitro drug-drug interaction assessment. Biomol. 2024;14(1):99. doi:10.3390/biom14010099.
33. Bhatt S, Dhiman S, Kumar V, Gour A, Manhas D, Sharma K, Ojha PK, Nandi U. Assessment of the CYP1A2 inhibition-mediated drug interaction potential for pinocembrin using in silico, in vitro, and in vivo approaches. ACS Omega. 2022;7(23):20321–20331. doi:10.1021/acsomega.2c02315.
34. Kanacher T, Lindauer A, Mezzalana E, Michon I, Veau C, Mantilla JDG, Nock V, Fleury A. A physiologically-based pharmacokinetic (PBPK) model network for the prediction of CYP1A2 and CYP2C19 drug–drug–gene interactions with fluvoxamine, omeprazole, s-mephenytoin, moclobemide, tizanidine, mexiletine, ethinylestradiol, and caffeine. Pharmaceutics. 2020;12(12):1191. doi:10.3390/pharmaceutics12121191.

